

## **SUPPORT INFORMATION**

### **Quantification of Drive-Response Relationships Between Residues During Protein Folding**

Yifei Qi and Wonpil Im

Department of Molecular Biosciences and Center for Bioinformatics, The University of Kansas, 2030 Becker Drive Lawrence, Kansas 66047, United States

## S1. Transfer entropy (TE) in three numerical systems

Our implementation of TE calculation was verified with the following three numerical systems.<sup>1</sup>

#1. A unidirectional linear process

$$\begin{aligned}x_i &= 0.8x_{i-1} + n_i^{(x)}(\sigma_x^2) + ey_{i-1} \\y_i &= 0.4y_{i-1} + n_i^{(y)}(\sigma_y^2)\end{aligned}$$

where  $e \in [0,1]$  is the coupling strength;  $n_i^{(x)}$  and  $n_i^{(y)}$  are independent Gaussian random process with zero mean and variance of  $\sigma_x^2 = \sigma_y^2 = 0.2$ . The system was simulated for  $2 \times 10^4$  steps and only the last  $10^4$  steps were used for calculation. By construction,  $y_i$  drives  $x_i$ , and the calculated  $D_{y \rightarrow x}$  is shown in Figure S1A.

#2. A unidirectional Henon map

$$\begin{aligned}x_i &= a - x_{i-1}^2 + b_x x_{i-2} \\y_i &= a - \{ex_{i-1} + (1-e)y_{i-1}\}y_{i-1} + b_y y_{i-2}\end{aligned}$$

where  $e \in [0,1]$  is the coupling strength; coefficients  $a$ ,  $b_x$ , and  $b_y$  were set to 1.4, 0.3 and 0.3. We simulated  $2 \times 10^5$  steps and only kept the last  $10^5$  steps for analysis. By construction,  $x_i$  drives  $y_i$ , and the calculated  $D_{y \rightarrow x}$  is shown in Figure S1B.

#3. A unidirectional Ulam map lattice

$$\begin{aligned}x_i^{(l)} &= f(ex_{i-1}^{(l-1)} + (1-e)x_{i-1}^{(l)}) \\f(x) &= 2 - x^2, l = 1, \dots, L\end{aligned}$$

where  $e \in [0,1]$  is the coupling strength, and  $L$ , the number of maps in the lattice, was fixed to 100. The last map is connected to the first one using the periodic boundary condition. We simulated  $2 \times 10^5$  steps and used the last  $10^5$  steps to analyze the interactions from the second map  $x_i^{(2)}$  to the first one  $x_i^{(1)}$ . By construction,  $x_i^{(1)}$  drives  $x_i^{(2)}$ , and the calculated  $D_{x_i^{(2)} \rightarrow x_i^{(1)}}$  is shown in Figure S1C.

For all TE calculations, the embedding dimension was set to 1 and the time series were symbolized to 4 symbols using even partition. In all the numerical systems, TE captured the drive/response relationship successfully (**Figure S1**). In the linear process (#1), the driving interaction increases as the coupling strength increases. In the Henon map (#2), the driving interaction drops quickly after  $e = 0.7$ , due to the synchronization of the two maps. In the Ulam map lattice (#3), the lattice undergoes two bifurcations where the driving interaction from  $x_i^{(1)}$  to  $x_i^{(2)}$  disappears.<sup>2</sup>

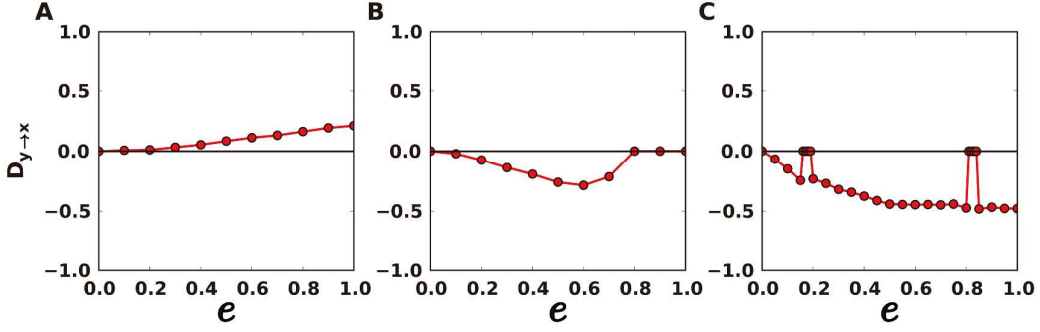


**Figure S1.** TE from  $y_i$  to  $x_i$  for (A) unidirectional linear process and (B) Henon map, from  $x_i^{(2)}$  to  $x_i^{(1)}$  for (C) unidirectional Ulam map lattice. A positive  $D_{y \rightarrow x}$  value indicates a drive interaction, while a negative value indicates a response interaction.

### S2. Driving and responding residues and MI for BBL, Villin and BBA

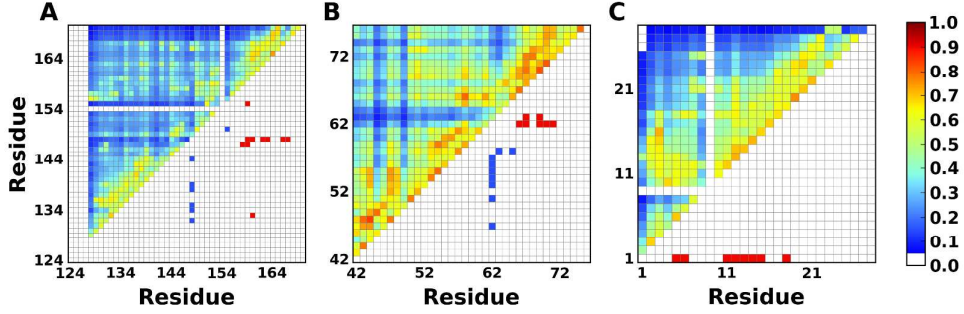


**Figure S2.** Driving and responding residues and MI of residue pairs in (A) BBL, (B) Villin and (C) BBA. In the lower-half triangle, red indicates that a residue from x-axis drives a residue from y-axis, blue indicates that a residue from x-axis responds to a residue from y-axis. MI was calculated from the whole trajectory (upper-half triangle). Values are colored from blue to red. MI values smaller than 0.05 are colored white.

### S3. Time-delayed mutual information (TDMI) in three numerical systems and folding trajectories

Introducing a time delay to equation (6) in the main text, we get the normalize TDMI:

$$MI'(x-t, y) = \sqrt{1 - e^{-2MI(x-t, y)}} \in [0, 1]$$

$$MI'(x, y-t) = \sqrt{1 - e^{-2MI(x, y-t)}} \in [0, 1]$$

Where  $MI()$  is the commonly used mutual information as in equation (5) in the main text. Similar to TE, we calculated the difference of TDMI between two directions,

$$TDMI_{y \rightarrow x} = MI'(x-t, y) - MI'(x, y-t) \in [-1, 1]$$

We used the same partition method as TE calculation and the time delay  $t$  was set to 1. In all the three numerical systems in Section S1, TDMI yielded very similar results to TE (**Figure S3**). However, when we applied TDMI to residues in the folding trajectories, it failed to give any information on the drive/response relationship, i.e., the information from both direction were too close and they canceled each other (**Figure S4**).

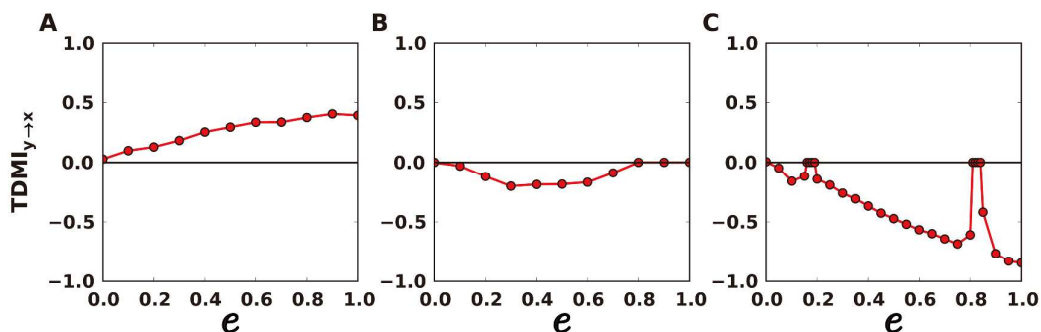


**Figure S3.** TDMI from  $y_i$  to  $x_i$  for (A) unidirectional linear process and (B) Henon map, from  $x_i^{(2)}$  to  $x_i^{(1)}$  for (C) unidirectional Ulam map lattice.

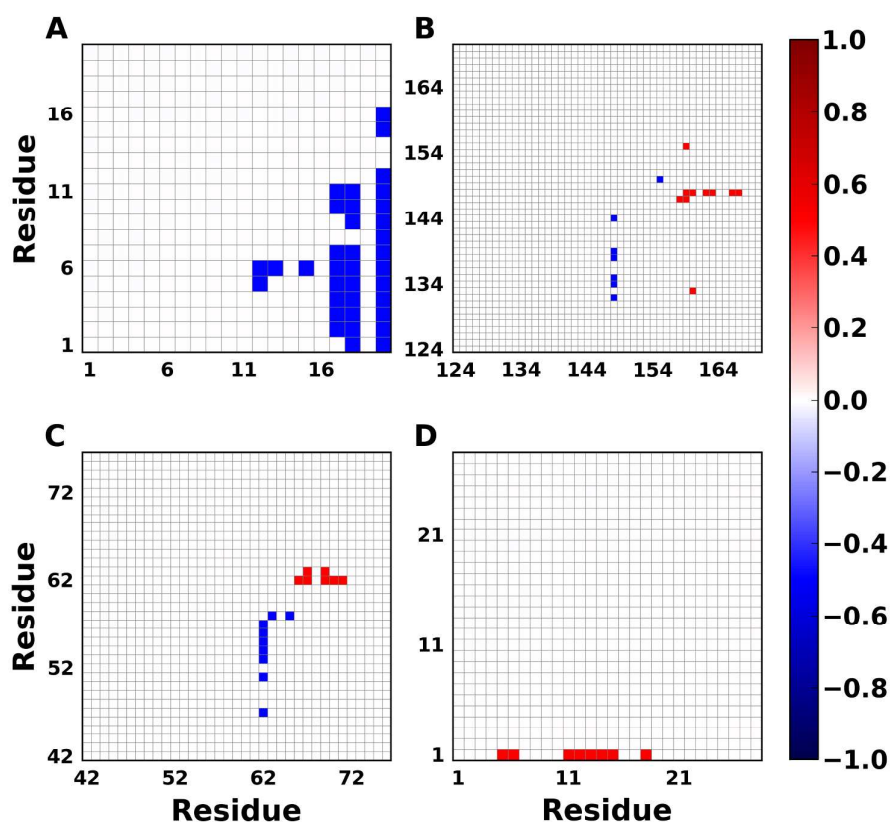


**Figure S4.** Driving and responding residues and TDMI of residue pairs in (A) Trp-cage, (B) BBL, (C) Villin and (D) BBA. In the lower-half triangle, red indicates that a residue from x-axis drives a residue from y-axis, blue indicates that a residue from y-axis drives a residue from x-axis.

from x-axis responds to a residue from y-axis. TDMI is colored from blue (-1) to red (1), but the values are too close to 0 and are all white (upper-half triangle).

#### S4. Coarse-grained simulation of protein L

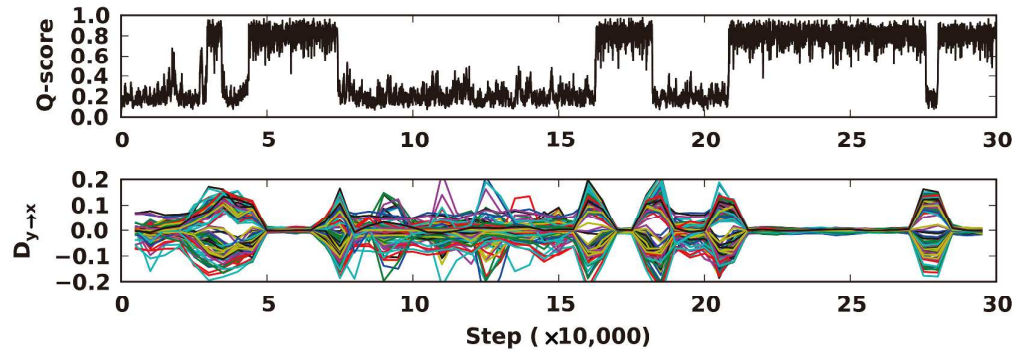


**Figure S5.** Q-score and  $D_{y \rightarrow x}$  profiles of protein L from a coarse-grained simulation.

#### References

- (1) Lungarella, M.; Ishiguro, K.; Kuniyoshi, Y.; Otsu, N., Methods for quantifying the causal structure of bivariate time series. *Int. J. of Bifurcation and Chaos* **2007**, *17*, 903-921.
- (2) Schreiber, T., Measuring information transfer. *Phys. Rev. Lett.* **2000**, *85*, 461-464.